Supporting Information

Bis(hexamethylazatriangulene)sulfone: A high-stability deep blue-violet fluorophore with 100% quantum yield and CIE$_y$ < 0.03

By Christopher M. Tonge,[1] Jiajie Zeng,[2] Zujin Zhao,[2,]* Ben Zhong Tang,[2,3] and Zachary M. Hudson[1,]*

[1] *Department of Chemistry, The University of British Columbia, 2036 Main Mall, Vancouver, British Columbia, Canada, V6T 1Z1.*
Tel: +1-604-822-3266; Fax: +1-604-822-2847; e-mail: zhudson@chem.ubc.ca.
[2] *State Key Laboratory of Luminescent Materials and Devices, Key Laboratory of Luminescence from Molecular Aggregates of Guangdong Province, South China University of Technology, Guangzhou 510640, China. E-mail: mszjzhao@scut.edu.cn*
[3] *Department of Chemistry, The Hong Kong University of Science & Technology, Clear Water Bay, Kowloon, Hong Kong, China*

Table of contents

Experimental Details

General Considerations:

All reactions and manipulations were carried out under a nitrogen atmosphere using standard Schlenk or glove box techniques unless otherwise stated. Dry solvents were obtained from Caledon Laboratories, dried using an Innovative Technologies Inc. solvent purification system, collected under vacuum, and stored under a nitrogen atmosphere over 4 Å molecular sieves. All reagents were purchased from Sigma-Aldrich or Alfa Aesar and used as received unless otherwise stated. HMAT and HMAT-Br were synthesized according to literature procedures.[1] The ^{1}H and $^{13}C\{^{1}H\}$ nuclear magnetic resonance (NMR) spectra were measured on a Bruker AV III HD 400 MHz spectrometer with dichloromethane-*d*$_2$ (CD_2Cl_2) as the solvent. Absorbance measurements were made on a Cary 60 spectrometer and fluorescence measurements were made on an Edinburgh Instruments FS5 spectrofluorometer. Absolute photoluminescence quantum yields were determined using an Edinburgh Instruments SC–30 Integrating Sphere Module; toluene was used as the solvent and spectra obtained at concentrations of 10^{-5} M. Two-photon cross-sections (σ_2) were calculated using the two-photon excited fluorescence method. Two-photon cross-section (σ_2) values from 710–850 nm were measured with an inverted two-photon fluorescence scanning microscope (Zeiss LSM 510 MP). Samples (3 mL) were measured in quartz cuvettes and concentrations were adjusted to give similar 2PEF intensities (**HMAT$_2$SO$_2$**, 6.0×10^{-5} M; **HMAT$_2$SO**, 6.0×10^{-5} mg mL^{-1}; **TBPA-DPS**, 1.3×10^{-4} M in toluene) and

Rhodamine B in MeOH (2.1 × 10^{-4} M in MeOH) was used as the reference.[2] The cuvette was illuminated at a depth of 0.6 mm from the bottom of the cuvette and imaged with a 10x/0.3 objective lens and femtosecond laser with a tuning range of 710-850 nm. The dichroic mirror had a cut-off at 660. The square-dependence of the fluorescence intensity on laser power was periodically confirmed for all measured and σ_2 was calculated using the quantum yield obtained from one-photon excitation experiments. Transient PL decay spectra were measured using Quantaurus-Tau fluorescence lifetime measurement system (C11367-03, Hamamatsu Photonics Co., Japan). Mass spectra were recorded on a Bruker HCTultra PTM Discovery System using electrospray ionization.

Electrochemical Methods

Cyclic voltammograms were recorded using a BASi Epsilon Eclipse potentiostat at room temperature using a standard three-electrode configuration (working electrode: 3 mm diameter glassy carbon; reference electrode: RE-5B Ag/AgCl electrode in saturated aqueous KCl (BASi Inc.), referenced externally to ferrocene/ferrocenium (0.543 V in 1,2-difluorobenzene);[3] counter electrode: Pt wire) in 0.2 M tetrabutylammonium hexafluorophosphate in 1,2-difluorobenzene with 2 mg mL^{-1} of sample. Experiments were run at a scan rate of 50 mV s^{-1} in dry degassed electrolyte solution with ~4 mg mL^{-1} of analyte. The HOMO level was found by referencing the oxidation peak to ferrocene and using the known HOMO of ferrocene (–4.80 eV) to calculate HOMO of **$HMAT_2SO$** and **$HMAT_2SO_2$** The LUMO level was calculated by subtracting the optical energy bandgap (E_g) from the HOMO value determined above. E_g was determined from the low-energy UV-absorption band edge.

Density Functional Theory

Quantum-mechanical calculations were performed using the Gaussian 16 Rev. B.01 computational package using default settings unless stated otherwise. All calculations were performed at the B3LYP/6-31+G(d) level of theory.[4]

X-Ray Crystallography

Single colorless flake-shaped crystals of **HMAT$_2$SO$_2$** were recrystallized from CH_2Cl_2 by slow evaporation. A suitable crystal 0.28×0.15×0.03 mm^3 was selected and mounted on a mylar loop in oil on a Bruker APEX II area detector diffractometer. The crystal was kept at a steady T = 100(2) K during data collection. The structure was solved with the XT[5] structure solution program using the Intrinsic Phasing solution method and by using Olex2[6] as the graphical interface. The model was refined with version 2017/1 of XL[7] using Least Squares minimization. CCDC 1960706.

Photobleaching

Photobleaching measurements were done on an inverted microscope. Sample aliquots (5 µL) were measured in a clear flat-bottom 1536-well plate (Greiner Bio One, Kremsmünster, Austria) with the wells covered with universal optical sealing tape (#6575, Corning). Sample concentrations were adjusted to obtain similar initial fluorescence intensities (**HMAT$_2$SO$_2$**, 0.001 mg mL^{-1}; **HMAT$_2$SO**, 0.0005 mg mL^{-1}; **TBPA-DPS**, 0.001 mg mL^{-1}). A 2 × 2 array of wells was illuminated and imaged with a 4× objective lens (NA 0.16). The excitation filter was 350/50 (center wavelength and bandwidth in nm), the dichroic mirror had a cut-off at 425 nm, and no emission filter was used. The excitation power was estimated to be ~98 mW at the sample. Samples were continuously illuminated using the above conditions and images were acquired at 1 min intervals for 90 min and analyzed using ImageJ[8] software with the Time Series Analyzer V3 plugin. The initial intensity for each sample was normalized to a value of unity.

OLED Fabrication and Characterization

Glass substrates with 90-nm indium tin oxide (ITO) with a sheet resistance of 15~20 Ω per square were successively cleaned in ultrasonic bath of acetone, isopropanol, detergent and deionized water, respectively, taking 10 minutes for each step, and then dried in a 70°C oven. Before the fabrication processes, the substrates were treated by O_2 plasma for 10 minutes. The OLED devices were fabricated under a pressure of $< 5 \times 10^{-4}$ Pa. Organic materials, LiF and Al were deposited at rates of 1~2 A s^{-1}, 0.1 A $s^{-1}$and 5 A s^{-1}, respectively.

The luminance–voltage–current density characteristics and electroluminescence spectra were obtained via a Photo Research PR-745 SpectraScan Spectroradiometer with a Keithley 2450 Source Meter. The external quantum efficiencies were estimated assuming that the devices are Lambertian emitters. The effective emitting area of the devices was 9 mm^2, determined by the overlap between anode and cathode. All the characterizations were conducted at room temperature in ambient conditions without any encapsulation, as soon as the devices were fabricated.

Synthetic Procedures:

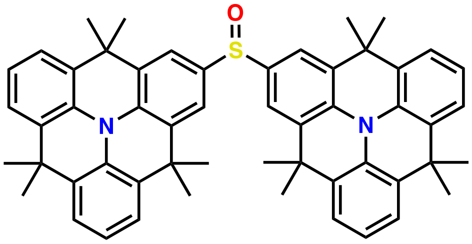

Synthesis of HMAT$_2$SO:

Prepared according to modified literature procedure.[9] A 250 ml Schlenk flask was charged flame dried then charged with 400 mg (0.9 mmol, 1 eq.) of HMAT-Br. The flask was sealed then evacuated and back filled three times with nitrogen. To this flask was added 100 mL of dry, degassed THF. The mixture was stirred at room temperature until all materials were fully dissolved. This mixture was then cooled to -78 ºC using a dry ice-acetone bath and allowed to equilibrate for 1 hour. Then, 0.62 mL of nBuLi (1.6 M in hexane, 0.99 mmol, 1.1 eq.) was added dropwise. The solution was then stirred for 1 hour at -78 ºC. To this lithiated mixture was added 49.5 mg of dimethyl sulfite (0.45 mmol, 0.5 eq.) dissolved in 5 mL of dry, degassed THF. The dimethyl sulfite was added dropwise over the course of 30 minutes. The reaction was allowed to stir for 1 hour at -78 ºC then allowed to warm to room temperature for 2 hours. The reaction was then quenched by dropwise addition of 10 mL of saturated aqueous NH_4Cl. The crude reaction mixture was then diluted with 200 mL of deionized water then extracted with dichloromethane (3 x 50 mL). The organic layer was pooled, dried on $MgSO_4$, filtered, then dried *in vacuo*. The crude mixture was purified on silica gel using a gradient from hexane to 1:1 hexane in dichloromethane. Yield 325 mg, 91%.

^{1}H NMR (400 MHz, Methylene Chloride-*d*$_2$): δ 7.64 (s, 4H), 7.41 – 7.34 (m, 8H), 7.14 (t, *J* = 7.7 Hz, 4H), 1.60 (s, 12H), 1.58 (s, 24H) ppm.

^{13}C NMR (101 MHz, Methylene Chloride-*d*$_2$): δ 139.3, 134.9, 131.6, 131.1, 130.7, 130.1, 124.5, 124.0, 123.8, 120.5, 36.2, 35.8, 33.7, 32.9 ppm.

HRMS (EIS) *m/z*: $[M]^{+\bullet}$ calcd for $[C_{54}H_{52}N_2OS]^{+\bullet}$, 776.3800; found, 776.3805; difference: -0.58 ppm.

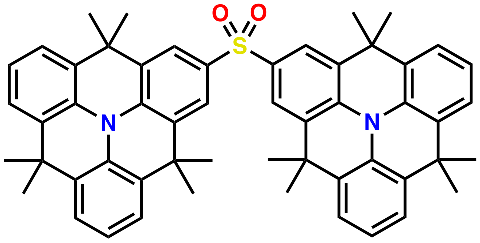

Synthesis of HMAT$_2$SO$_2$:

To a dry 100 mL round bottom flask was added 656 mg (0.83 mmol, 1 eq.) of HMAT$_2$SO and 50 mL of dry dichloromethane. To this flask was added 428 mg of mCPBA (2.49 mmol, 3 eq.) once all starting material was dissolved. The reaction was monitored by TLC to determine at what point the reaction was complete. Once complete, the reaction was quenched by addition of 30 mL of saturated Na_2CO_3 in water followed by diluting the crude reaction with 100 mL of deionized water. The mixture was then extracted three times with 50 mL of dichloromethane. The organic layer was then dried over MgSO4, filtered, and dried in vacuo. The crude reaction mixture was then purified over silica gel using a gradient from hexane to 1:1 hexane:dichloromethane to yield the desired product. X-ray quality crystals were prepared by slow evaporation from hexanes/CH_2Cl_2. Yield 611 mg, 93%.

^{1}H NMR (400 MHz, Methylene Chloride-*d*$_2$): δ 7.90 (s, 4H), 7.43 – 7.34 (m, 8H), 7.16 (t, *J* = 7.7 Hz, 4H), 1.60 (d, *J* = 1.8 Hz, 36H) ppm.

^{13}C NMR (101 MHz, Methylene Chloride-*d*$_2$): δ 136.5, 135.8, 131.2, 130.9, 130.5, 130.2, 124.7, 124.3, 123.7, 122.5, 36.1, 35.7, 33.9, 32.6 ppm.

HRMS (ESI) *m/z*: $[M]^{+\bullet}$ calcd for $[C_{54}H_{52}N_2O_2S]^{+\bullet}$, 792.3749; found, 792.3758; difference: -1.02 ppm.

Additional Figures:

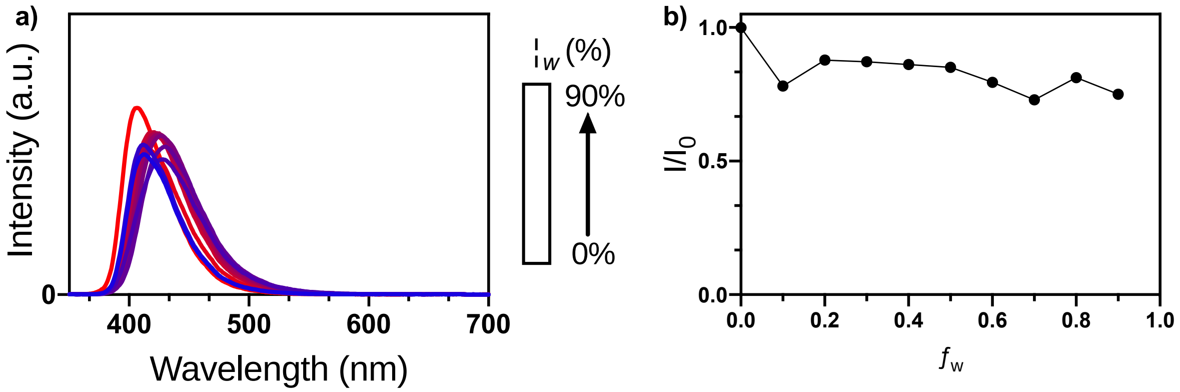

Figure S1. a) Aggregation induced emission spectra for **HMAT$_2$SO$_2$** from 0% water in THF to 90% water in THF, measured at 0.025 mg mL^{-1}; b) Plot of I/I$_0$ for HMAT$_2$SO$_2$ from $f_w = 0$ to $f_w = 0.9$ where I$_0$ is the intensity at λ_{max} when fw = 0 and I is intensity at λ_{max}.

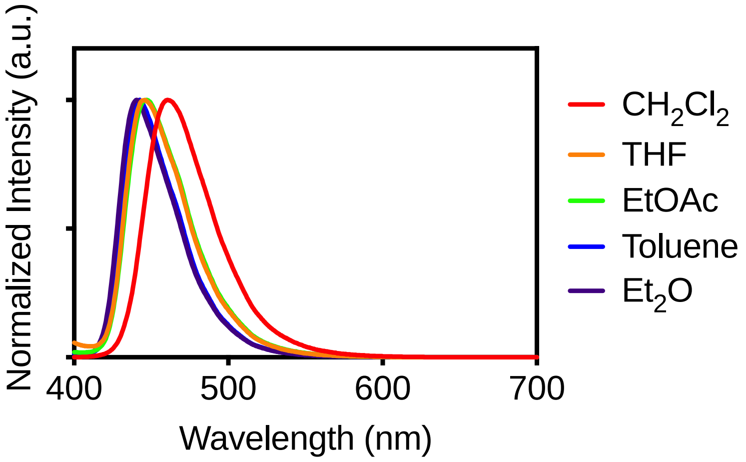

Figure S2. Photoluminescence spectra for **HMAT$_2$SO$_2$**; measured at 0.01 mg mL^{-1} in various solvents.

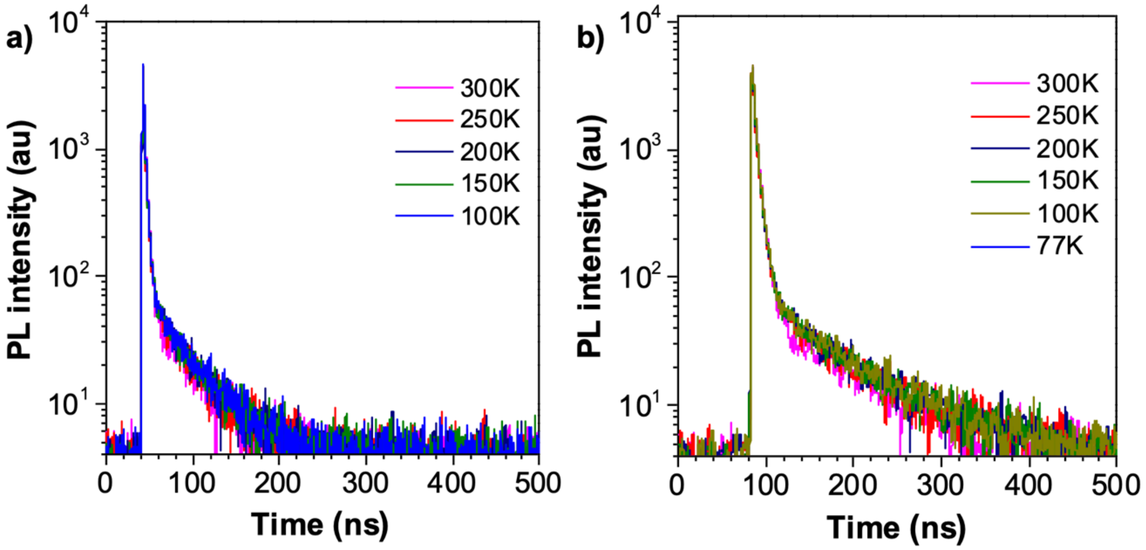

Figure S3. Temperature-dependent fluorescence lifetimes of **a) HMAT$_2$SO$_2$** and **b) HMAT$_2$SO** measured as spin-cast films, excited at 340 nm.

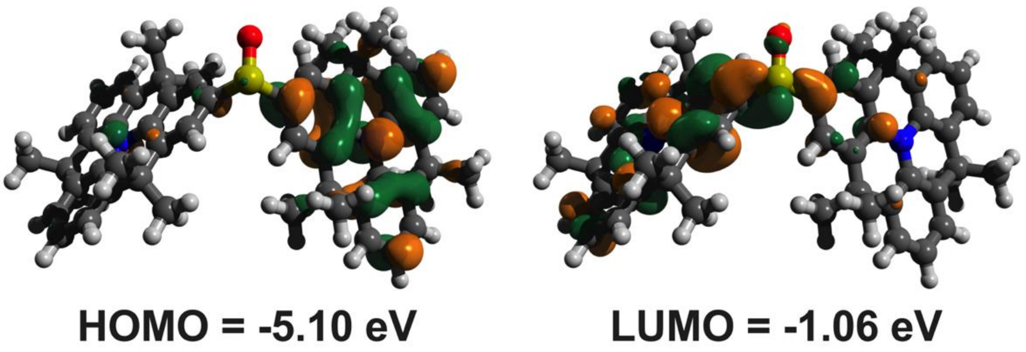

Figure S4. Calculated HOMO and LUMO diagrams for **HMAT$_2$SO**.

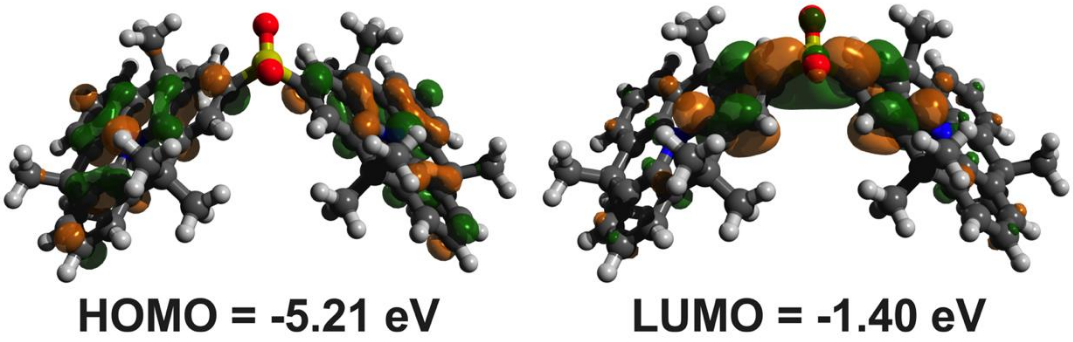

Figure S5. Calculated HOMO and LUMO diagrams for **HMAT$_2$SO$_2$**.

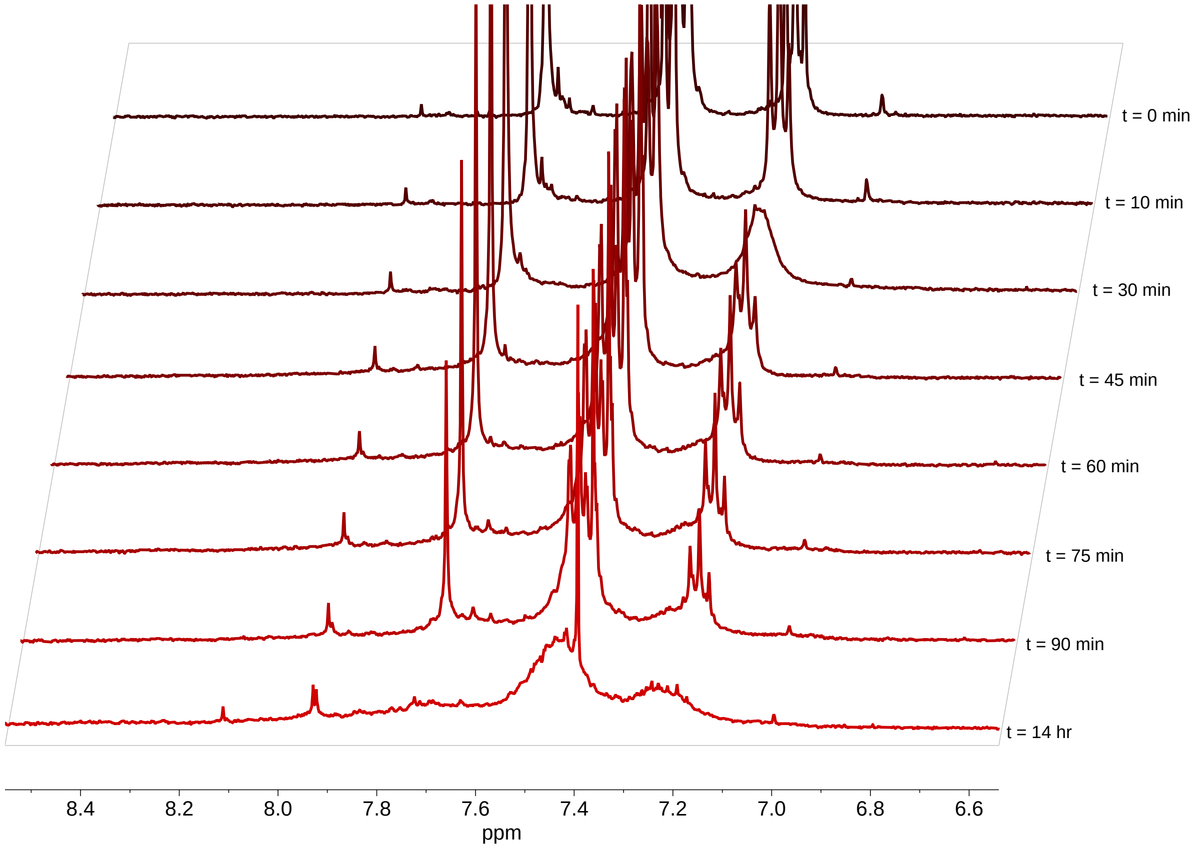

Figure S6. Time series progression of NMR aliquots of **HMAT$_2$SO** while continuously irradiating at 365 nm. Measurements were taken every 15 minutes for 90 minutes and again after 14 hours. Spectra were measured in CD_2Cl_2 at a concentration of 2 mg mL^{-1}.

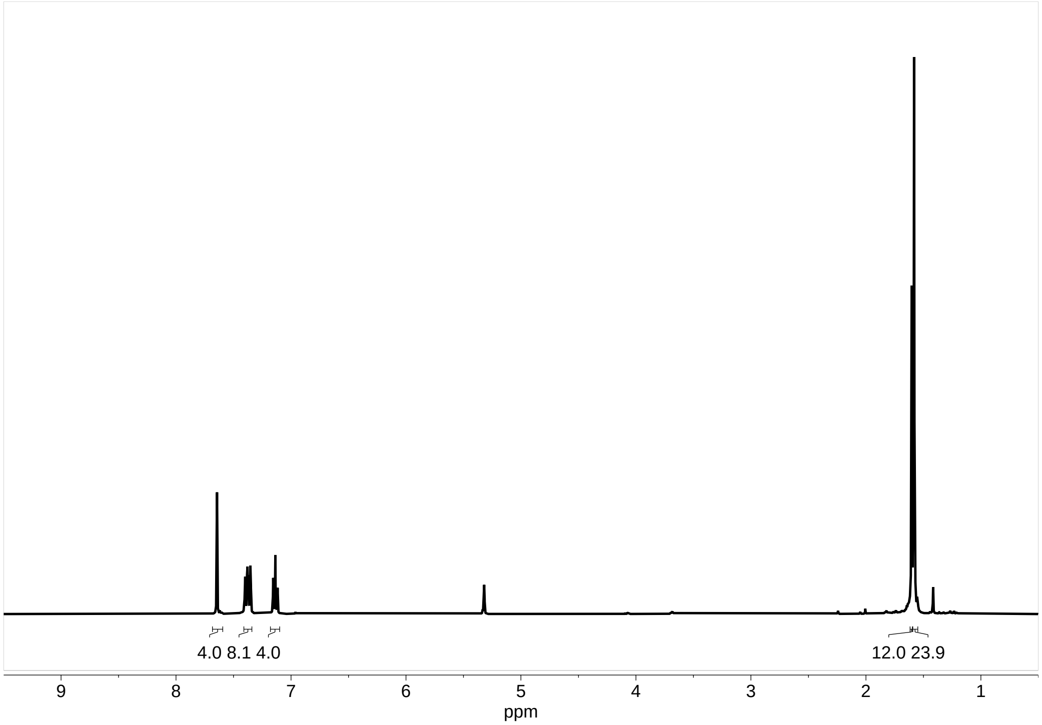

Figure S7. ^{1}H NMR spectrum of **HMAT$_2$SO** in CD_2Cl_2.

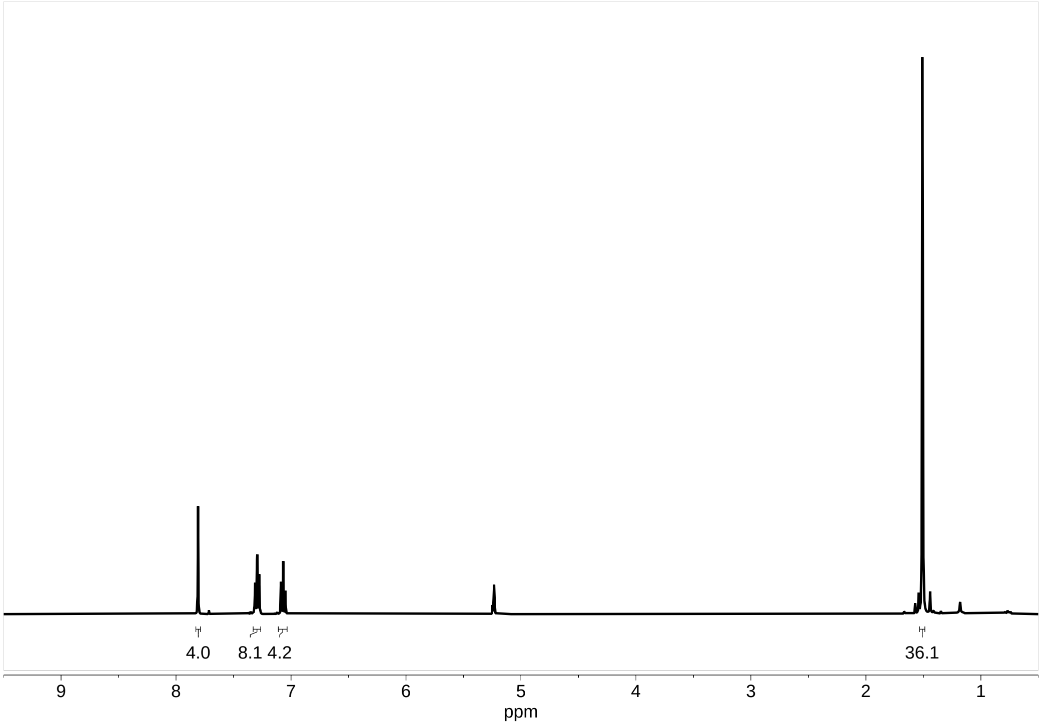

Figure S8. ^{1}H NMR spectrum of **HMAT$_2$SO$_2$** in CD_2Cl_2.

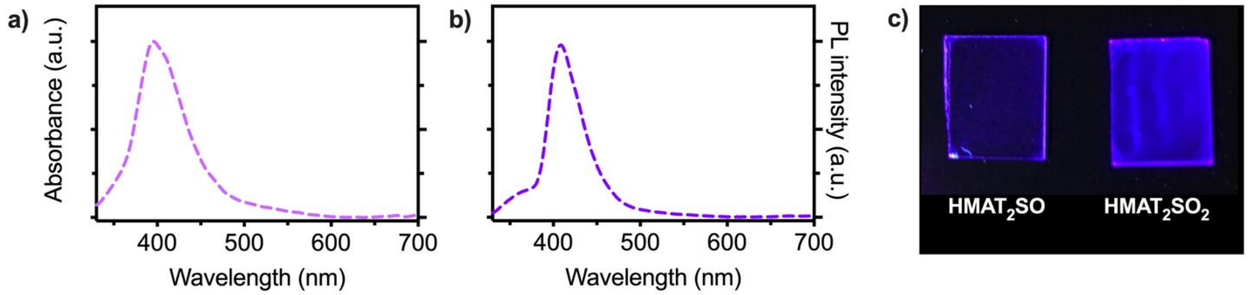

Figure S9. Emission spectra for a) **HMAT$_2$SO** and b) **HMAT$_2$SO$_2$** prepared as a 1% doped film in PMMA, cast as a thin film on a glass slide; c) Photographs of the films prepared under illumination at 365 nm.

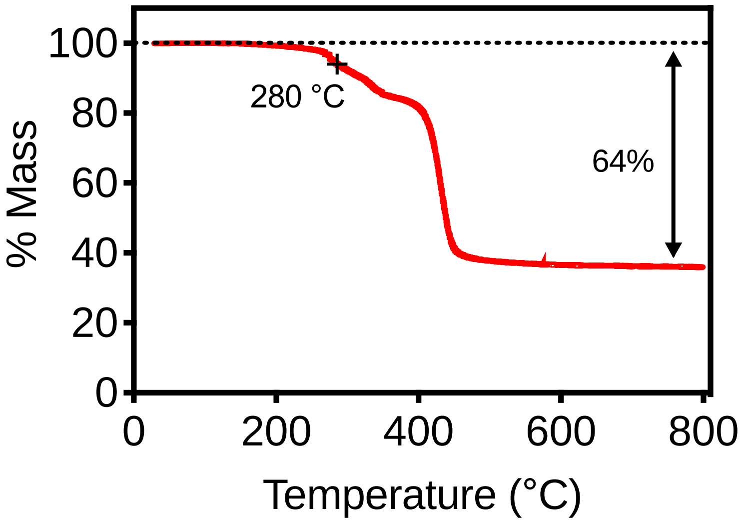

Figure S10. Thermogravimetric analysis of **HMAT$_2$SO$_2$** (5.9 mg), run at a rate of 10 °C min^{-1} under a 50 mL min^{-1} flow of nitrogen from 25 to 800 °C.

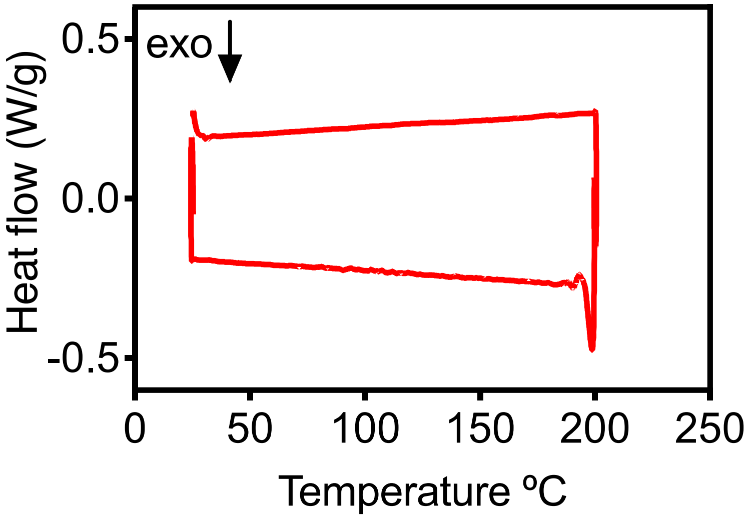

Figure S11. DSC traces of **HMAT$_2$SO$_2$** run at a rate of 10 °C min^{-1} under a 50 mL min^{-1} flow of nitrogen. Three consecutive heating and cooling cycles were performed, the second is shown above.

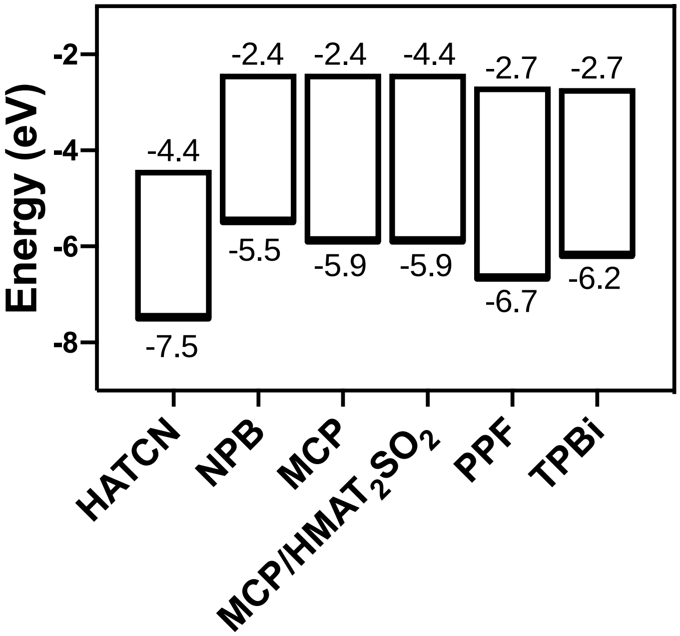

Figure S12. Diagram of the device structure used for OLEDs **I-IV.**

Table S1. Fluorescence lifetimes vs. temperature for **HMAT$_2$SO$_2$** measured as a neat film under nitrogen.

Temperature	τ_{total}	τ_1	τ_2	τ_3
	ns			
100K	10.2	1.37	3.25	43.9
150K	10.0	1.16	3.25	41.2
200K	10.6	1.06	3.17	43.3
250K	9.90	0.935	3.26	42.1
300K	9.48	1.25	3.25	46.7

Table S2. Fluorescence lifetimes vs. temperature for **HMAT$_2$SO** measured as a neat film under nitrogen.

Temperature	τ_{total}	τ_1	τ_2
	ns		
77K	1.18	0.820	3.25
100K	1.17	0.828	3.23
150K	1.22	0.819	3.12
200K	1.21	0.815	3.08
250K	1.25	0.792	3.32
300K	1.16	0.760	3.12

Table S3. Progress of conversion of **HMAT$_2$ SO** to **HMAT$_2$SO$_2$** under UV irradiation at 365 nm in CD_2Cl_2

Time (min)	Integral 7.64 ppm **(HMAT$_2$SO)**	Integral 7.90 ppm **(HMAT$_2$SO$_2$)**	Conversion to **HMAT$_2$SO$_2$**
0	1	0	0%
10	1	0.07	6.5%
30	1	0.08	7.4%
45	1	0.17	14.5%
60	1	0.25	20%
75	1	0.33	25%
90	1	0.39	28%

Table S4. Crystallography data for solid-state structure of compound **HMAT$_2$SO$_2$**.

Formula	$C_{54}H_{52}N_2O_2S$
$D_{calc.}$/ g cm^{-3}	1.301
μ/mm^{-1}	0.127
Formula Weight	793.03
Colour	colourless
Shape	flake
Size/mm^3	0.28×0.15×0.03
T/K	100(2)
Crystal System	monoclinic
Space Group	$P2_1/c$
a/Å	14.6045(6)
b/Å	10.5284(4)
c/Å	26.4015(11)
α/°	90
β/°	94.3480(10)
γ/°	90
V/Å^3	4047.9(3)
Z	4
Z'	1
Wavelength/Å	0.71073
Radiation type	MoK$_\alpha$
Θ_{min}/°	1.398
Θ_{max}/°	28.308
Measured Refl.	46632
Independent Refl.	10051
Reflections with I > 2(I)	6835
R_{int}	0.0673
Parameters	637
Restraints	1627
Largest Peak	0.598
Deepest Hole	-0.404
GooF	1.005
wR_2 (all data)	0.1417
wR_2	0.1249
R_1 (all data)	0.0962
R_1	0.0567

Table S5. Electroluminescent Data for **$HMAT_2SO_2$** at higher doping concentrations.

	λ_{EL} (nm)^e	V_{on} (V)^d	L (cd/m^2)^c	η_C (cd/A)^c	η_P (lm/W)^c	EQE (%)^c	CIE (x, y)^e
I^a	420	3.6	341	0.49	0.40	0.73	(0.175, 0.091)
II^b	428	3.5	102	0.39	0.31	0.30	(0.207, 0.186)

[a] ITO/HATCN (5 nm)/TAPC (20 nm)/mCP (5 nm)/20 wt% CT-6-11: mCP (20 nm)/TmPyPB (55 nm)/LiF (1 nm)/Al (120 nm)

[b] ITO/HATCN (5 nm)/TAPC (20 nm)/mCP (5 nm)/CT-6-11 (20 nm)/TmPyPB (55 nm)/LiF (1 nm)/Al (120 nm)

[c] The luminescence (L), current efficiency (η_c), power efficiency (η_P) and external quantum efficiency are the maximum values of the devices.

[d] V_{on} is the turn-on voltage at 1 cd/m^2.

[e] Electroluminescence peak (λ_{EL}) and CIE coordinates at 5V.

Table S6. Photophysical properties of **$HMAT_2SO_2$** and **$HMAT_2SO$** in the solid state.

Emitter	**$HMAT_2SO$**	**$HMAT_2SO_2$**
$\lambda_{max,em}$^{a}	395 nm	410 nm
CIE^a	(0.187,0.112)	(0.175,0.064)
FWHM^a	65 nm	45 nm

[a] Measured in a PMMA film (1% doping concentration by weight) spin cast on a glass slide.

References

1 Z. Fang, T. L. Teo, L. Cai, Y. H. Lal, A. Samoc and M. Samoc, *Org. Lett.*, 2009, **11**, 1–4.

2 N. S. Makarov, M. Drobizhev and A. Rebane, *Opt. Express*, 2008, **16**, 4029.

3 J. R. Aranzaes, M.-C. Daniel and D. Astruc, *Can. J. Chem.*, 2006, **84**, 288–299.

4 Gaussian 16 Rev B.01, M. J. Frisch, G. W. Trucks, H. B. Schlegel, G. E. Scuseria, M. A. Robb, J. R. Cheeseman, G. Scalmani, V. Barone, B. Mennucci, G. A. Petersson, H. Nakatsuji, M. Caricato, X. Li, H. P. Hratchian, A. F. Izmaylov, J. Bloino, G. Zheng, J. L. Sonnenberg, M. Hada, M. Ehara, K. Toyota, R. Fukuda, J. Hasegawa, M. Ishida, T. Nakajima, Y. Honda, O. Kitao, H. Nakai, T. Vreven, J. A. Montgomery Jr., J. E. Peralta, F. Ogliaro, M. Bearpark, J. J. Heyd, E. Brothers, K. N. Kudin, V. N. Staroverov, R. Kobayashi, J. Normand, K. Raghavachari, A. Rendell, J. C. Burant, S. S. Iyengar, J. Tomasi, M. Cossi, N. Rega, J. M. Millam, M. Klene, J. E. Knox, J. B. Cross, V. Bakken, C. Adamo, J. Jaramillo, R. Gomperts, R. E. Stratmann, O. Yazyev, A. J. Austin, R. Cammi, C. Pomelli, J. W. Ochterski, R. L. Martin, K. Morokuma, V. G. Zakrzewski, G. A. Voth, P. Salvador, J. J. Dannenberg, S. Dapprich, A. D. Daniels, Ö. Farkas, J. B. Foresman, J. V Ortiz, J. Cioslowski and D. J. Fox, *Gaussian Inc.*, 2016, Wallingford CT.

5 G. M. Sheldrick, *Acta Crystallogr. Sect. A Found. Adv.*, 2015, **71**, 3–8.

6 O. V. Dolomanov, L. J. Bourhis, R. J. Gildea, J. A. K. Howard and H. Puschmann, *J. Appl. Crystallogr.*, 2009, **42**, 339–341.

7 G. M. Sheldrick, *Acta Crystallogr. Sect. C Struct. Chem.*, 2015, **71**, 3–8.

8 C. A. Schneider, W. S. Rasband and K. W. Eliceiri, *Nat. Methods*, 2012, **9**, 671–675.

9 J. Yuan, P. R. Christensen and M. O. Wolf, *Chem. Sci.*, 2019,**10**, 10113-10121.